AD-A164 685 MOLECULAR JET STUDY OF THE SOLVATION OF TOLUENE BY METHANE ETHANE AND PROPANE(U) COLORADO STATE UNIV FORT COLLINS DEPT OF CHEMISTRY M SCHAUER ET AL. 15 JAN 85 1/1

UNCLASSIFIED TR-15 N00014-79-C-0647 F/G 7/4 NL

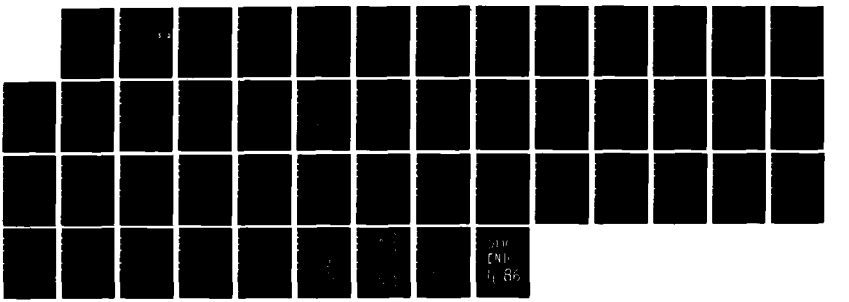

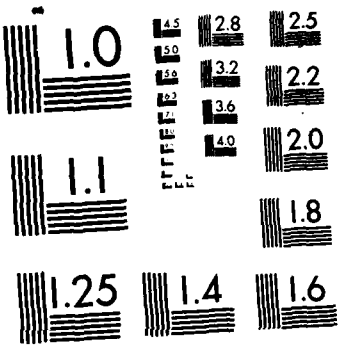

MICROCOPY RESOLUTION TEST CHART
NATIONAL BUREAU OF STANDARDS-1963-A

AD-A164 685

(12)

OFFICE OF NAVAL RESEARCH

Contract N00014-79-C-0647

TECHNICAL REPORT #15

MOLECULAR JET STUDY OF THE SOLVATION OF TOLUENE BY METHANE, ETHANE, AND PROPANE

DTIC
ELECTE
FEB 19 1986
S D

by

Mark Schauer, K.S. Law and E.R. Bernstein

Prepared for Publication
in the
Journal of Chemical Physics

Department of Chemistry
Colorado State University
Fort Collins, Colorado 80523

January 15, 1985

Reproduction in whole or in part is permitted for any purpose of the United States Government

This document has been approved for public release and sale; its distribution is unlimited.

DTIC FILE COPY

86 2 19 004

SECURITY CLASSIFICATION OF THIS PAGE *(When Data Entered)*

REPORT DOCUMENTATION PAGE		READ INSTRUCTIONS BEFORE COMPLETING FORM
1. REPORT NUMBER Technical Report #15	2. GOVT ACCESSION NO. AD-A164 685	3. RECIPIENT'S CATALOG NUMBER
4. TITLE *(and Subtitle)* Molecular Jet Study of the Solvation of Toluene by Methane, Ethane, and Propane		5. TYPE OF REPORT & PERIOD COVERED Technical Report 6. PERFORMING ORG. REPORT NUMBER
7. AUTHOR(s) Mark Schauer, K.S. Law and E.R. Bernstein		8. CONTRACT OR GRANT NUMBER(s) N00014-79-C-0647
9. PERFORMING ORGANIZATION NAME AND ADDRESS Colorado State University Department of Chemistry Fort Collins, CO 80523		10. PROGRAM ELEMENT, PROJECT, TASK AREA & WORK UNIT NUMBERS
11. CONTROLLING OFFICE NAME AND ADDRESS Chemistry Program, Materials & Science Division Office of Naval Research, 800 N. Quincy Street Arlington, Virginia 22217		12. REPORT DATE January 15, 1985 13. NUMBER OF PAGES 43
14. MONITORING AGENCY NAME & ADDRESS*(if different from Controlling Office)*		15. SECURITY CLASS. *(of this report)* Unclassified 15a. DECLASSIFICATION/DOWNGRADING SCHEDULE

16. DISTRIBUTION STATEMENT *(of this Report)*

This document has been approved for public release and sale; its distribution is unlimited.

17. DISTRIBUTION STATEMENT *(of the abstract entered in Block 20, if different from Report)*

18. SUPPLEMENTARY NOTES

19. KEY WORDS *(Continue on reverse side if necessary and identify by block number)*

20. ABSTRACT *(Continue on reverse side if necessary and identify by block number)*

Two color time of flight mass spectroscopy studies of toluene solvated by methane, ethane, and propane in a supersonic molecular jet have been carried out. This work is quite similar to the studies in the preceding paper on benzene: the conclusions and finding in the benzene investigation are strengthened and elaborated. The comparison of calculations and experiments has yielded information on binding energy, geometry and spectral shift. A strong correlation is found between observed cluster transition intensity and cluster

DD FORM 1 JAN 73 1473 EDITION OF 1 NOV 65 IS OBSOLETE

SECURITY CLASSIFICATION OF THIS PAGE *(When Data Entered)*

20. nucleation processes and a tentative nucleation scheme for the molecular jet formation of solute-solvent clusters is presented.

I. INTRODUCTION

The spectroscopic study of van der Waals (vdW) clusters in a molecular jet supersonic expansion has greatly increased our understanding of these species. Additionally, clusters composed of an aromatic molecule (solute) surrounded by small hydrocarbons (solvent) have been discussed as models for condensed phase systems.[1] Initial studies of these models have been focused on relatively small clusters with few solvent molecules:[2] geometries, energetics, and energy dynamics have all been explored in these vdW systems.

In a companion paper (here after referred to as I), information on benzene solvated with methane, ethane, and propane is presented.[4] Based on this and previous work from our laboratory, the nature of solvation and the solvation process has been explored. The solvent shift in the benzene clusters is understood to arise primarily from the interaction of the solvent with the π-cloud of the aromatic ring: hence, the strong dependence of spectral shift on geometry. Identification of cluster geometry and energy levels has also led to understanding of the nucleation processes important in the formation of van der Waals clusters. Homogeneous nucleation can occur through the vibrational predissociation (VP) of a solvent dimer as it forms a complex with the aromatic solute. Inhomogeneous nucleation (the addition of two or more solvent molecules at a time to a solute) can be the dominant process in the beam: the relative amount of homogeneous and inhomogeneous nucleation is proportional to the ratio of solvent-solvent binding energy to solvent-solute binding energy.

Availability Codes
Dist Avail and/or Special
A-1

The present paper reports the results of a study of the vdW clusters of toluene with methane, ethane, and propane. Due to the reduction of the solute symmetry compared to benzene, the geometry and energetics of toluene clusters are different from those of benzene clusters. Comparison of the benzene and toluene results for similar beam conditions and the same solvents strengthens and generalizes the conclusions reached previously.

Both large ($tol(S)_x$, $x>3$) and small ($x<3$) clusters have been studied for the toluene solvent systems. The changes in the spectra of these clusters as larger and larger clusters are probed indicate possible relationships between the clusters and condensed phase systems. Comparisons of the large cluster spectra with the spectra of cryogenic solutions[6] suggest how well and to what extent the jet generated clusters model condensed phase systems.

Computer modeling of toluene-hydrocarbon clusters is extremely helpful in supplementing the small cluster spectroscopic data in order to determine cluster geometry and binding energy. A number of local minima are found in the potential surface for toluene interacting with these hydrocarbon solvents: only the lowest energy computer generated geometries which are consistent with the observed spectra are taken as acceptable solute-solvent configurations. If the computer generated potential energy surface has a number of minima with relatively low energy, that geometry which best agrees with the toluene and benzene spectra is accepted as the appropriate one.

The toluene cluster data will be discussed in two parts.The data for small clusters will be analyzed first and will be compared to the benzene small cluster data. The modeling of condensed phase systems by large clusters will be dealt with at the end of the Discussion Section.

II EXPERIMENTAL PROCEDURES

The apparatus and techniques employed in this work are similar to those described in I. Mass selective absorption (2-color MS) is the only spectroscopic technique used in this study. The optimal backing conditions for each nozzle are found experimentally and are reported in the figure captions.

Three different nozzles are used in these experiments. The pulsed nozzle with a 500 μm orifice produced a factor of ∿15 larger intensity than the 50 μm continuous (CW) nozzle which in turn produces signals 3 to 4 times more intense than the 25μm CW nozzle. Greater enhancements in the signals were expected for the larger diameter nozzles;[7] several possible loss mechanism may contribute to this reduced signal improvement. In general, however, direct comparison between signals from the various nozzles is difficult because the optimum backing conditions for clustering are different for each nozzle.

Lowering the backing pressure and raising the pulsed nozzle temperature reduces the cooling in the expansion and produces hot clusters which evidence spectral hot bands. Although the (calculated) translational temperature of the expansion at the most extreme warming conditions (P_o = 10 psi, T_o = 70°C) is still quite low (∿1K),[8] the vibrational temperature of the clusters is ∿50 to 100K based on

the observed spectral intensities. Calculations of the minimum energy configurations of toluene clusters are performed as described in I. The coefficients for the interactions between the methyl group of toluene and the solvents are taken to be the same as those between solvents. The coefficients are reproduced in Table I for convenience.

Minimization of the energy of a given cluster is accomplished by moving the ligands in a stepwise fashion, calculating the energy at each step, and comparing the two most recent values of the energy. The procedure will terminate each time a local minimum in the energy has been found. To ensure that all minima are found and, in particular, that the lowest minimum is located, all reasonable starting geometries must be employed. Low energy and agreement with the spectroscopic data are the two criteria used to settle on "correct" configurations for the clusters.

III RESULTS

Toluene-Methane

The $Tol(CH_4)_{1,2}$ absorption spectra have been published previously and are reproduced here in figure 1 and Table II for convenience. These spectra exhibit sharp origins and features due to van der Waals (vdW) stretching and bending modes. The spectral shift for the $Tol(CH_4)_2$ 0_0^0 is twice that of the $Tol(CH_4)_1$ 0_0^0. The additive shift indicates addition of the two methane molecules to equivalent sites on the toluene. The stretching mode for $Tol(CH_4)_1$ has a considerable anharmonicity as pointed out previously.[5] $Tol(CH_4)_2$ evidences a similar progression in the stretching mode. The $Tol(CH_4)_2$ peak at -20 cm^{-1} is probably associated with a second configuration of $Tol(CH_4)_2$.

Larger clusters of toluene with methane produce broad spectra which become more diffuse and structureless as the clusters increase in size (see figure 2). The red shift of the most prominent feature in the $Tol(CH_4)_3$ spectrum is non-additive; this feature is actually less red shifted than the $Tol(CH_4)_2$ 0_0^0. Nonetheless, intensity is still evident in the $Tol(CH_4)_3$ spectrum far to the red of the $Tol(CH_4)_2$ 0_0^0.[5] The absorption spectra of clusters as large as $Tol(CH_4)_{10}$ have been observed. The spectra become very broad and unstructured with a maximum about -50 cm^{-1} from the Tol 0_0^0.

The binding energy of these clusters can be estimated by observing the presence or absence of higher vibronic bands in the 2-color MS spectra. If the first photon induces a transition to a level which results in vibrational predissociation of the cluster, the transition will not be observed in the 2-color MS spectrum.[9] For $Tol(CH_4)_{1,2}$ the $6b_0^1$ transition is observed but the 1_0^1 transition is not. This sets the limits on the binding energy at $534 \leq D_0 \leq 740$ cm^{-1}.

The binding energy is the same within these limits for $Tol(CH_4)_{1,2}$. The binding energy for larger clusters is difficult to estimate since the spectra of large clusters are less well defined and weak.

The computer modeling of $Tol(CH_4)_1$ shows a minimum energy configuration in which the methane is shifted away from the center of the aromatic ring toward the methyl group (see figure 3, Table III). The methane should interact strongly with the aromatic π-cloud of toluene in this predicted geometry. Only one stable configuration is calculated for $Tol(CH_4)_1$: this agrees with the observation of one origin in the spectrum. The calculated binding energy of 667 cm^{-1} is

consistent with the limits obtained spectroscopically.

Two acceptable geometries are found in the computer modeling of $Tol(CH_4)_2$. The configuration labeled I in figure 3 features a methane on either side of the aromatic ring, forming an isotropic cluster. The second configuration predicted by the computer modeling (labeled II in figure 3) is anisotropic with both methane molecules on the same side of the ring. In the isotropic geometry both of the solvent molecules occupy equivalent sites similar to the site occupied by methane in $Tol(CH_4)_1$. Consequently, this geometry should have the larger (additive) spectral shift in the $Tol(CH_4)_2$ spectrum (figure 1).

Toluene-Ethane

The small clusters of toluene and ethane ($Tol(C_2H_6)_{1,2}$) exhibit sharp, assignable structure (see figure 4 and Table IV). $Tol(C_2H_6)_1$ shows a long progression in the vdW stretch, as well as two intense bends. The $Tol(C_2H_6)_2$ spectrum clearly suggests that two geometries exist for this cluster. One geometry generates a spectral shift which is twice that found for $Tol(C_2H_6)_1$. The vdW vibrational features of this additive shift configuration consist of long progressions in the stretching mode. The second geometry is characterized by a small (-10 cm^{-1}) solvent shift and a short progression of doublets after the origin peak. The absorption spectra of larger $Tol(C_2H_6)_x$ clusters become broad with very little well-defined structure. The maximum in a typical absorption spectrum occurs at about 30 cm^{-1} to the low energy side of the Tol 0_0^0, although significant measurable intensity extends to roughly -200 cm^{-1}.

The effect of warming the $Tol(C_2H_6)_x$ clusters is similar to

that of warming the $Tol(CH_4)_x$ clusters. The hot bands produce a broad background somewhat to the low energy side of the cold bands. As judged by the decrease in the signal intensities, continued warming (P < 20 psi, T_o $\sim 70^oC$) begins to destroy the vdW complexes.

Vibrational predissociation of $Tol(C_2H_6)_{1,2}$ clusters occurs at the 12^1 toluene excitation but not at 1^1: the binding energy of these clusters therefore lies between 740 and 933 cm^{-1}. Both geometries of $Tol(C_2H_6)_2$ seem to have the same binding energy within this experimentally defined range.

The computer modeling of $Tol(C_2H_6)_1$ shows two minima in the potential surface above toluene. Since only one geometry is obvious experimentally only the lower energy computer generated configuration is presented in figure 5 and Table V. The less stable geometry (~ 180 cm^{-1} higher in energy) is probably not observed spectroscopically, although one of the peaks assigned to a vdW bending mode is possibly the origin of a second configuration. The binding energy predicted by the computer modeling is within the spectroscopically determined limits.

For $Tol(C_2H_6)_2$ several possible geometries are calculated. Since the spectrum clearly shows only two geometries, the most probable configurations must be chosen from this group. One of the geometries must be an isotropic configuration with an ethane on either side of the ring and the other configuration must involve both ethane molecules on the same side of the ring. Configurations consistent with the spectrum are shown in figure 5.

Toluene-Propane

The spectra of the small clusters of toluene and propane ($Tol(C_3H_8)_{1,2,3}$) also consist of well resolved features (figure 6 and Table VI). The $Tol(C_3H_8)_1$ cluster spectrum strongly suggests two configurations exist for this cluster. The geometry with a relatively large spectral shift shows a progression in the vdW stretch as well as several vdW bends to the high energy side of its 0_0^0 transition. The second configuration gives rise to a small spectral shift of the origin: the origin is followed by a progression of doublets. This pattern is quite reminiscent of that found for the second (small shift) configuration of $Tol(C_2H_6)_2$.

The vdw cluster spectrum of $Tol(C_3H_8)_2$ has a complicated structure indicating three or four possible different configurations for this mass species. These geometries are generally distinguishable based on relative intensities, spectral shifts, qualitative vibrational analysis, and comparison with the $Tol(CH_4)_{1,2}$, $Tol(C_2H_6)_{1,2}$, and $Tol(C_3H_8)_1$ data.

The $Tol(C_3H_8)_3$ spectrum is actually less congested than the $Tol(C_3H_8)_2$ spectrum, presumably because some of the possible configurations are not observed in the beam. Two sets of peaks, corresponding to two different geometries of $Tol(C_3H_8)_3$, are present in the spectrum as shown in figure 6. One set of peaks features a regular progression in an apparently single vdW mode and the other features a short progression of doublets.

Warming the toluene-propane clusters destroys the well-resolved structure in the $Tol(C_3H_8)_{2,3}$ spectra (figure 7); as in the other systems, hot bands of the $Tol(C_3H_8)_x$ clusters form an unstructured, broad background to the red of the cold spectrum.

The large, clusters of toluene and propane produce spectra

qualitatively similar to those of the other systems (figure 8). Although some structure exists in the $Tol(C_3H_8)_4$ spectrum, the $Tol(C_3H_8)_6$ spectrum is largely unstructured with an intensity maximum around -60 cm^{-1} relative to the Tol 0_0^0.

The binding energies of the $Tol(C_3H_8)_{1,2,3}$ clusters are all greater than 933 cm^{-1} as all three clusters show clear spectra in the 12_0^1 region. No toluene features above 12_0^1 are either intense enough or free enough from interferences to allow further studies; therefore, no upper limit to the binding energy can be quoted at this time.

Computer modeling predicts several stable geometries for $Tol(C_3H_8)_1$. As noted earlier, the $Tol(C_3H_8)_1$ spectrum indicates that two configurations with very different spectral shifts exist (see figure 6). Note the similarity in the spectral shifts of configuration II of $Tol(C_3H_8)_1$ and configuration II of $Tol(C_2H_6)_2$ (figure 4). This similarity in spectral shift indicates a similarity in the overlap of the solvent with the aromatic ring of toluene. Figure 9 and Table VII present the lowest energy geometries which should give rise to spectral shifts consistent with the $Tol(C_3H_8)_1$ spectrum base on the correspondence between solvent-aromatic ring overlap and spectral shift (I). Other less stable geometries may be producing some of the observed peaks in the spectrum, but further assignments cannot be made with the existing data.

Similar considerations are used to choose those geometries of $Tol(C_3H_8)_2$ which are consistent with the spectrum. These minimum energy geometries are pictured in figure 10 and tabulated in Table VIII. Computer modeling of $Tol(C_3H_8)_3$ was not done.

IV DISCUSSION

The spectral shift of a cluster depends primarily on the polarizability of the solvent along the intermolecular bond and on the change in polarizability of the solute upon excitation. One would expect that the change in polarizability upon excitation is larger for toluene than benzene and thus, that the cluster shifts are larger for toluene than benzene clusters. However, most of the change in polarizability upon (π-π^*) excitation occurs in the aromatic π-system; moving the solvent away from the π-system must significantly reduce the cluster shift. Thus, two competing effects, increased polarizability change and reduced interaction with the aromatic π-system, influence the relative spectral shifts of benzene and toluene clusters with small hydrocarbons. In the ensuing discussion we will treat large and small clusters separately and discuss shifts, geometries, and nucleation processes.

A. Small Clusters.

Methane

The computer modeling of the $Tol(CH_4)_1$ cluster shows that the methane is displaced 0.921Å towards the methyl group of toluene (see figure 3, Table III). This calculated geometry presents a rational for the essential (unexpected) equivalence of the cluster spectral shifts for $Tol(CH_4)_1$ and $Ben(CH_4)_1$, even though toluene has a (presumed) larger change in polarizability upon excitation than does benzene. Thus, the above mentioned two competing effects tend to cancel one another for $Tol(CH_4)_1$.

These basic ideas also help to rationalize the similarities and

differences in the $Tol(CH_4)_2$ and $Ben(CH_4)_2$ spectra. Spectra of the isotropic clusters (a solvent on each side of the aromatic ring) of $Tol(CH_4)_2$ and $Ben(CH_4)_2$ are nearly identical, as would be surmised based on the above arguments for the $Tol(CH_4)_1$ clusters. However, anisotropic clusters of toluene and benzene with two methanes exhibit significantly different shifts. Computer modeling of the anisotropic cluster of $Ben(CH_4)_2$ suggests that only one methane moiety interacts strongly with the π-system (I), thus yielding a spectral shift similar to that observed for $Ben(CH_4)_1$. On the other hand, computer modeling of the anisotropic cluster of $Tol(CH_4)_2$ shows that both methane molecules are considerably displaced from the center of the aromatic ring (1.09Å and 2.37Å). The observed small spectral shift for $Tol(CH_4)_2$ ($-21 cm^{-1}$) is thereby consistent with the previously determined (I) relationship between spectral shift and geometry.

The ratios of intensities of the isotropic to anisotropic cluster peaks are different for $Tol(CH_4)_2$ and $Ben(CH_4)_2$: I_{iso}/I_{aniso} $[Tol(CH_4)_2, 0_0^0]$ $\sim$3 (figure 1), whereas I_{iso}/I_{aniso} $[Ben(CH_4)_2, 6_0^1]$ $\sim$1. As pointed out in I, isotropic clusters can only be produced by homogeneous nucleation. Most homogeneously nucleated clusters are argued to form through the collision of a solvent dimer with the solute; the binding energy of the solute with one of the solvent molecules is dissipated, in part, by VP of the solvent dimer bond. Apparently, the larger solute-solvent binding energy of the toluene clusters (as predicted by the computer modeling) facilitates breaking of the solvent dimer bond and allows homogeneous

nucleation to dominate the formation of $Tol(CH_4)_2$ clusters. Nucleation processes will be treated in more detail at the end of this section.

Ethane

Figure 5 depicts the computer calculated geometry for $Tol(C_2H_6)_1$: the ethane molecule is displaced toward the methyl group of toluene and inclined with respect to the plane of the ring. Assuming this geometry to be correct, it results in a spectral shift smaller by roughly 5 cm^{-1} than that found for the comparable $Ben(C_2H_6)_1$ configuration. The methyl group of toluene, according to the potential calculations, draws the ethane solvent molecule away from the ring center, thereby reducing the toluene spectral shift relative to the comparable benzene cluster.

An isotropic $Tol(C_2H_6)_2$ cluster is clearly indicated in the observed spectrum based on an origin shift twice that of the $Tol(C_2H_6)_1$ origin (figure 4). The intensity of features due to isotropic clusters relative to those due to anisotropic clusters is much less than seen in the $Tol(CH_4)_2$ spectrum. The ratio is consistent with the trend report in I; homogeneous nucleation can be less probable with solvents having larger binding energies than with solvents having smaller binding energies. However, more homogeneous nucleation is evident for the toluene-ethane system than for the benzene-ethane system: this same trend was found for the solute-methane clusters and is related to the strength of the solvent-solute bond.

Propane

Arguments put forth above concerning spectral shift, solvent-solute geometry, binding energies, etc., can also be applied for the somewhat more complicated toluene-propane clusters. The spectral shifts of the two configurations determined by computer modeling of $Tol(C_3H_8)_1$ (figure 9) can thereby be qualitatively predicted. Configuration I, having a significant interaction of a terminal methyl group of propane with the aromatic π-system of toluene, should have a spectral shift greater than that of $Tol(CH_4)_1$. On the other hand, configuration II (figure 9) would be expected to have a small spectral shift since the propane molecule is close to the methyl group of toluene. Origins with the expected shifts are indeed observed in the spectrum of $Tol(C_3H_8)_1$ as depicted in figure 6.

The $Tol(C_3H_8)_2$ spectrum (figure 6) has substantial intensity tentively assigned to isotropic clusters (see origin peaks labled I, II, III in Table VI and figure 10: although it is also possible that configurations II and III may be anisotropic. This observation apparently does not fit the trend established above if the computer predicted values of the solvent dimer and solute-solvent binding energies are used. However, computer modeling of the propane dimer suggests that several geometries are stable, some of which have relatively small binding energies. If a reasonable fraction of the propane dimers in the beam are hot or are in geometries with small binding energies (i.e. ca. 500 cm^{-1}), the relative number of isotropic clusters in the beam would be larger than otherwise expected.

Nucleation

The nucleation process in the jet expansion can be better understood by employing a simple kinetic scheme. We assume, as has been previously suggested (I), that small vdW clusters are formed by solute collisions with solvent dimers (or possibly larger species). While this may not be the only cluster formation mechanism, it is consistent with all benzene and toluene cluster data and can be justified by reasonability arguments. A solvent dimer colliding with the solute produces an "activated complex" in much the same fashion as is typically considered in a bimolecular reaction. This complex can then decay through three different pathways: 1) vibrational predissociation of the solvent dimer to form a homogeneously nucleated solute $(solvent)_1$ vdW cluster; 2) collision with a third body (He, typically) to generate a inhomogeneously nucleated solute $(solvent)_2$ vdW cluster; or 3) decay back to the reactants $(solvent)_2$ and solute.

Data presented in the Results Section indicate that details of the solvent dimer binding energy and solute-solvent binding energy are important for the relative concentrations of homogeneously and inhomogeneously nucleated products. Thus, finer detail in the overall kinetic scheme should be considered. The mechanism suggested for the reaction is represented as follows:

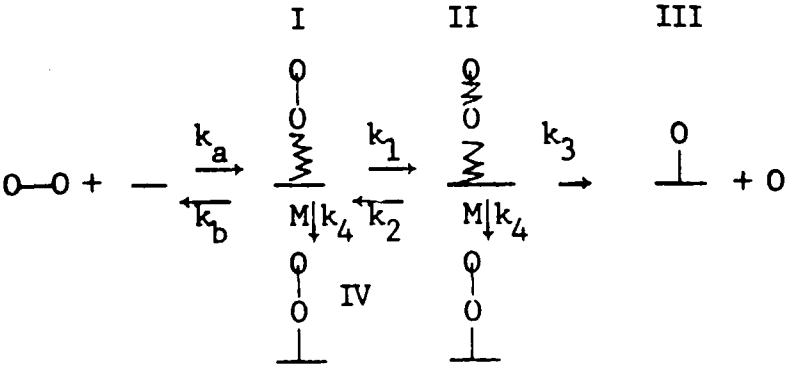

Tol(CH4)3
Tol(CH4)4
Tol(CH4)6
0
-50
-100
RELATIVE ENERGY (WAVENUMBERS)

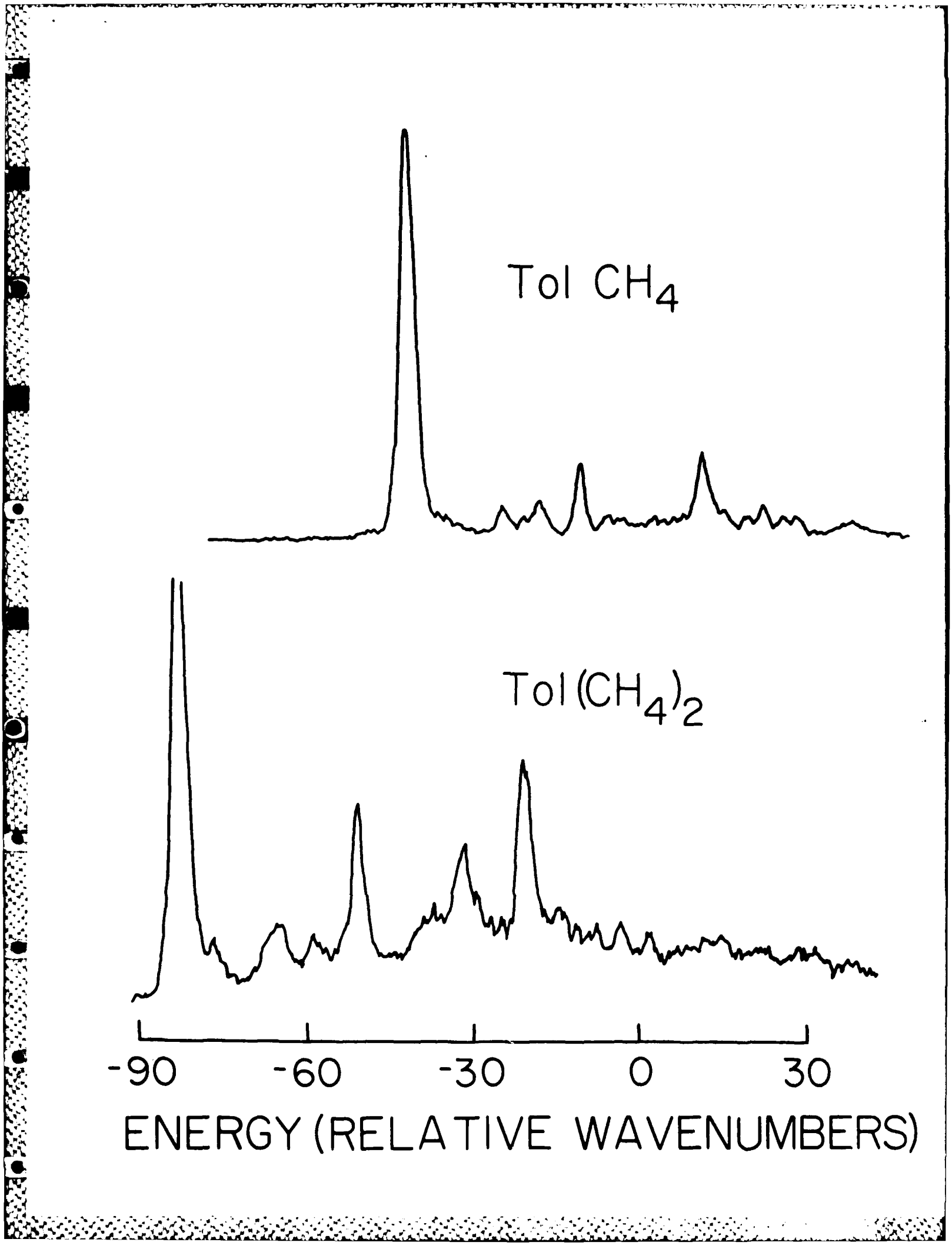
Tol CH_4
Tol $(CH_4)_2$
-90
-60
-30
0
30
ENERGY (RELATIVE WAVENUMBERS)

in which ~~~ indicates a vdW bond with significant vibrational excitation, O indicates a solvent molecule, M stands for an inert third-body collision partner and — represents the solute. Assuming $d[II]/dt=0$, and ignoring the first step in the reaction chain, the ratio of concentrations [IV] to [III] is given by

$$\frac{[IV]}{[III]} \propto \frac{k_4}{k_3} \frac{(k_1+k_2+k_3+k_4)}{k_1} \qquad (1)$$

The amount of inhomogeneous nucleation relative to homogeneous nucleation is proportional to this ratio. Two reasonable approximations can be made for this expression. First, $k_4 < k_1, k_2$ as k_4 is at most $\sim 10^{11}$ sec^{-1} in the backing region (and certainly much less in the beam) while $k_1, k_2 \sim 10^{12}$ sec^{-1}. If this were not the case, inhomogeneously nucleated clusters would always dominate the intensity. Second, $k_1 \simeq k_2$ because the density of states is high for both species at the given energies (300-900 cm^{-1}) and energy is not expected to concentrate in one bond or the other over many vibrational periods. With these approximations equation (1) becomes

$$\frac{[IV]}{[III]} \propto \frac{k_4}{k_3} \qquad (2)$$

k_4 depends only on the collision rate of third bodies with the species I and II and should be roughly the same for all the systems studied here. The difference in the relative numbers of isotropic species for the various systems must then be associated with the changes in k_3 from cluster to cluster.

The transformation of species II to species III can be viewed as a reaction with a potential barrier equal to the binding energy of the solvent dimer. The rate constant k_3 can be written as

$$k_3 \sim \exp [-BE_{LL}/E_{LL}]. \qquad (3)$$

in which BE_{LL} is the solvent dimer binding energy and E_{LL} is the energy in the solvent dimer bond for species II. If equilibrium is established ($k_1, k_2 >> k_3$) before VP occurs and the excess energy in the intermediate is statistically distributed between the solvent-solute and solvent-solvent bonds, then $E_{LL} \sim \frac{1}{2} BE_{SL}$, in which BE_{SL} is the solute-solvent binding energy. This latter quanity takes on the role of kT for the reaction II→ III. Thus k_3 becomes a function of both the solvent-solvent and solute-solvent binding energies. Table IX shows that the relative number of isotropic clusters in the system scales approximately with this form for k_3. Of course, the detailed behavior of the ratio [III]/[II] depends on the appropriateness of the various approximations for each system.

B. Large Clusters

The intensity <u>maximum</u> in the spectrum of clusters with more than three solvent molecules is much less red shifted with respect to the free molecule than the intensity <u>maximum</u> in the comparable cryogenic solution.[5] This observation is directly attributable to the conditions of the experiment and the nature of the nucleation processes in the expansion. Inhomogeneous nucleation dominates the formation of large clusters, especially for clusters

involving better solvents such as propane. Since inhomogeneous nucleation produces more anisotropic clusters, most of the large clusters formed in the jet will be anisotropic and will exhibit small spectral shifts; larger spectral shifts are found for isotropic (solution-like) clusters.

The spectral shifts in the jet generated clusters have been determined to be largely due to interaction between the solvent and the aromatic π-system of the solute. If the clusters are to serve as potential models of condensed phase systems, the difference between the principal gas to cluster and gas to liquid shifts must be explored. [Note nonetheless, that some cluster intensity is found at the same spectral shift as that observed for the analogous solution.[1,4,5]] While in general the shifts for clusters are saturated with a solvent molecule on each side of the aromatic ring, larger shifts might arise through two mechanisms: forced crowding of the solvent around the solute so that more molecules effectively interact with the π-system of the solute, and interaction of the solvent with the solute in the plane of the ring. These latter positions are not local minima in the potential surface of small clusters. However, the cage structure of the liquid would force solvent molecules to interact with the solute in the ring plane. This in-plane interaction may also contribute to the spectral shift of larger vdW clusters and, in particular, could be responsible for the weak intensity at approximately the value of the solution spectral shift reported for these systems previously.[6] Since we have no direct information on the in-plane interactions, the relative contribution to the shift from these two possible sources is difficult to assess.

V. CONCLUSIONS

Two-color time of flight mass spectroscopy and simple potential calculations have been employed to determine cluster binding energy, spectral shift, geometry and nucleation processes for toluene solvated by methane, ethane and propane. The major findings of this effort can be summarized as follows:

1. Cluster binding energy is related to the polarizability of the two species in the cluster and is apparently not a sensitive function of solute-solvent geometry;

2. The observed spectral shift for a cluster is due mostly to the solvent interaction with the solute aromatic π-system and therefore is a sensitive function of cluster geometry;

3. The nucleation of clusters under the experimental beam conditions is suggested to occur through the interaction of solvent dimers or larger aggregates and the solute monomer - whether isotropic clusters (homogeneous nucleation) or anisotropic clusters (inhomogeneous nucleation) arise depends on the relative size of the solvent dimer binding energy and the solute-solvent binding energy;

4. The benzene and toluene cluster systems appear to behave in a consistent and predictable fashion - the data analysis for both systems has been carried out such that trends are transferable from one system of clusters to another; and

5. The exponential-6,atom-atom potentials employed in the computer modeling of cluster geometry and binding energy, which have been quite successfully used over the years in treating condensed phases, are apparently reasonable potentials for the modeling of cluster.

ACKNOWLEDGMENT

We are grateful to Professor O. Anderson and C. Schauer for help with the computer simulated drawing and for use of the crystallographic computing system.

REFERENCES

1) See for example E.R. Bernstein, K. Law, and M. Schauer, J. Chem. Phys., 80, 634 (1984) and Ibid. 204 (1984) and references therein.

2) See for example A. Amirav, U. Even, and J. Jortner, J. Chem. Phys., 75, 2489 (1981).

3) See for example D.V. Brumbaugh, J.E. Kenny, and D.H. Levy, J. Chem. Phys., 78, 3415 (1983).

4) M. Schauer, K. Law, and E.R. Bernstein, J. Chem. Phys., preceding paper.

5) M. Schauer, K. Law, and E.R. Bernstein, J. Chem. Phys., in press.

6) J. Lee, F. Li, and E.R. Bernstein, J. Phys. Chem., 87, 1180 (1983).

7) O.F. Hagena, Molecular Beams and Low Density Gasdynamics, (Marcel Dekker, Inc., New York, 1974), Vol. 4, pp. 93-182.

8) J.B. Anderson, Ibid., pp. 1-92.

9) J.E. Kenny, K.E. Johnson, W. Sharfin, and D.H. Levy, J. Chem. Phys., 72, 1109 (1980).

10) R. Kaila, L. Dixit, and P.L. Gupta, Acta. Phys. Hung., 42, 237 (1977).

TABLE I

Parameters for the energy expression in the computer modeling of the vdW clusters of toluene.

$$E_{ij} = - A_{ij} / R_{ij}^{6} + B_{ij} \exp [- C_{ij} \quad R_{ij}]$$

	$A\left(\frac{cm^{-1}\,\text{Å}^{6}}{mole}\right)$	$B\left(\frac{cm^{-1}}{mole}\right)$	$C\ (\text{Å}^{-1})$
Aliphatic-Aliphatic[a]			
C-C	131096	8890353	3.421
C-H	47830	7562708	3.94
H-H	15028	6390528	4.643
Aliphatic-Aromatic[b]			
C-C	162645	16520286	3.5105
C-H	47864	6434085	3.805
H-H	13071	2497533	4.1915
Aromatic-Aromatic[c]			
C-C	201786	30698427	3.6
C-H	47897	5473891	3.67
H-H	11368	976084	3.74

a) From the methane-methane parameters of ref. 11 in paper I.

b) The parameters are found by combining the benzene-benzene and methane-methane parameters as follows:

$$A_{Bm} = (A_{BB}\, A_{mm})^{\frac{1}{2}}$$

$$B_{Bm} = (B_{BB}\, B_{mm})^{\frac{1}{2}}$$

$$C_{Bm} = \tfrac{1}{2}(C_{BB} + C_{mm})$$

c) From the benzene-benzene parameters of ref. 10 in paper I.

TABLE II

Two-color TOFMS of Tol(CH_4) and Tol(CH_4)$_2$ in the 0_0^0 region. Only the prominent peaks are tabulated and tentative assignments are given (see figure 1).

Species	Energy (vac. cm^{-1})	Energy relative to Tol 0_0^0	Energy relative to cluster 0_0^0	Assignment[a]
Tol(CH_4)				
	37434.4	-43	0	0_0^0
	37451.8		17	A_0^1
	37458.7		24	B_0^1
	37466.2		32	V_0^1
	37488.5		54	V_0^2
Tol(CH_4)$_2$ I				
	37394.1	-83	0	0_0^0
	37412.6		18	A_0^1
	37418.5		24	B_0^1
	37426.7		32	V_0^1
	37440.5		46	$V_0^1A_0^1$
	37446.2		52	V_0^2
II				
	37456.9	-21	0	0_0^0

a) Tentative assignments are as follows: V stands for the Tol-CH_4 stretch and A and B are different vdW bends. I and II represent different configurations.

TABLE III

The atomic positions for the minimum energy configurations of $Tol(CH_4)_1$ and $Tol(CH_4)_2$ (see figure 3). The origin is at the center of the aromatic ring of toluene. The + X axis passes through the methyl group, the Y axis is in the plane of the ring and the Z axis is out of the plane of the ring.

	Atom	X(Å)	Y(Å)	Z(Å)	Energy (cm^{-1})
Toluene					
	C1	2.925	0	0	
	C2	-1.395	0	0	
	C3	- .6975	1.208	0	
	C4	.6975	1.208	0	
	C5	1.395	0	0	
	C6	.6975	-1.208	0	
	C7	- .6975	-1.208	0	
	H1	3.29	0	-1.038	
	H2	3.29	.8985	.518	
	H3	3.29	- .8985	.518	
	H4	-2.479	0	0	
	H5	-1.24	2.147	0	
	H6	1.24	2.147	0	
	H7	1.24	-2.147	0	
	H8	-1.24	-2.147	0	
$Tol(CH_4)_1$					- 667
	C1	.921	0	3.384	
	H1	- .104	0	2.985	
	H2	1.451	- .8985	3.036	
	H3	1.451	- .8985	3.036	
	H4	.884	0	4.483	
$Tol(CH_4)_2$	Configuration I				-1348
Ligand 1	C1	.922	0	3.381	
	H1	- .103	0	2.982	
	H2	1.452	- .8985	3.033	
	H3	1.452	.8985	3.033	
	H4	.886	0	4.48	
Ligand 2	C1	.767	0	-3.391	
	H1	- .255	0	-2.983	
	H2	1.300	- .8985	-3.048	
	H3	1.300	.8985	-3.048	
	H4	.721	0	-4.49	

TABLE III
(continued)

	Atom	X(Å)	Y(Å)	Z(Å)	Energy (cm^{-1})
Configuration II					-1360
Ligand 1	C1	2.372	.003	3.433	
	H1	1.977	- .8968	2.938	
	H2	3.470	.005	3.371	
	H3	1.973	.900	2.938	
	H4	2.066	.003	4.490	
Ligand 2	C1	-1.089	- .003	3.454	
	H1	-2.172	- .005	3.260	
	H2	- .634	- .901	3.011	
	H3	- .638	.896	3.011	
	H4	- .913	- .003	4.540	

TABLE IV

Two-color TOFMS of $Tol(C_2H_6)_1$ and $Tol(C_2H_6)_2$. Only the prominent peaks are tabulated and tentative assignments are given (see figure 4).

Species	Energy (vac cm^{-1})	Energy origin relative to Tol 0_0^0 (cm^{-1})	Energy relative to cluster 0_0^0 (cm^{-1})	Assignment[a]
$Tol(C_2H_6)$				
	37435	-43	0	0_0^0
	37450		15	A_0^1
	37454		19	B_0^1
	37458		23	V_0^1
	37460		25	A_0^2
	37475		40	$V_0^2(V_0^1A_0^1)$
	37485		50	$V_0^1A_0^2$
	37486		51	V_0^3
$Tol(C_2H_6)_2$ I				
	37392	-86	0	0_0^0
	37411		19	V_0^1
	37428		36	V_0^2
	37445		53	V_0^3
	37461		69	V_0^4
	37478		86	V_0^5
II				
	37467	-11	0	0_0^0
	37481		14	A_0^1
	37489		22	B_0^1
	37492		25	V_0^1

a) Tentative assignments are as follows: V stands for the fundamental vdW stretch A and B are different vdW bends. I and II represent different geometries. In $Tol(C_2H_6)_2$ the vdW modes may involve solvent-solvent motions as well as solvent-solute motions.

TABLE V

The atomic positions for the minimum energy configurations of $Tol(C_2H_6)_1$ and $Tol(C_2H_6)_2$ (see figure 5). Axes and solute coordinates are the same as in Table III.

	Atom	X(Å)	Y(Å)	Z(Å)	Energy (cm^{-1})
$Tol(C_2H_6)_1$					- 967
Ligand	C1	.166	- .001	3.742	
	C2	1.672	- .001	3.478	
	H1	- .374	0	2.783	
	H2	- .104	.897	4.317	
	H3	- .105	- .900	4.315	
	H4	2.212	- .002	4.437	
	H5	1.943	.898	2.905	
	H6	1.942	- .899	2.903	
$Tol(C_2H_6)_2$	Configuration I				-1663
Ligand 1	C1	.017	.041	3.877	
	C2	1.515	.185	3.599	
	H1	- .524	- .051	2.924	
	H2	- .340	.929	4.418	
	H3	- .156	- .857	4.487	
	H4	2.056	.277	4.553	
	H5	1.688	1.083	2.989	
	H6	1.574	- .734	3.061	
Ligand 2	C1	.302	0	-3.845	
	C2	1.802	0	-3.541	
	H1	- .262	.001	-2.900	
	H2	.048	.898	-4.426	
	H3	.047	- .899	-4.425	
	H4	2.366	- .001	-4.486	
	H5	2.057	.899	-2.961	
	H6	2.056	- .898	-2.960	
Configuration II					-1834
Ligand 1	C1	- .628	1.561	3.933	
	C2	-1.263	.311	3.555	
	H1	-1.355	2.254	4.496	
	H2	- .336	2.187	3.018	
	H3	.261	1.471	4.554	
	H4	-1.554	- .226	4.469	
	H5	-2.151	.490	2.933	
	H6	- .535	- .292	2.991	

TABLE V
(continued)

	Atom	X(Å)	Y(Å)	Z(Å)	Energy (cm^{-1})
Ligand 2	C1	2.294	-1.263	3.754	
	C2	2.820	.157	3.538	
	H1	2.139	-1.748	2.778	
	H2	3.027	-1.838	4.338	
	H3	1.341	-1.221	4.299	
	H4	2.087	.732	2.953	
	H5	3.774	.115	2.993	
	H6	2.975	.642	4.513	

TABLE VI

Two-color TOFMS of $Tol(C_3H_8)_1$, $Tol(C_3H_8)_2$ and $Tol(C_3H_8)_3$. Only the prominent peaks are tabulated and tentative assignments are given (see figure 6).

Species	Energy (cm^{-1})	Energy origin relative to Tol 0_0^0 (cm^{-1})	Energy relative to cluster 0_0^0 (cm^{-1})	Assignment[a]
$Tol(C_3H_8)$ I				
	37419	- 59	0	0_0^0
	37433		14	A_0^1
	37435		17	B_0^1
	37440		22	C_0^1
	37442		24	D_0^1
	37448		30	V_0^1
	37452		33	$B_0^1A_0^1$
	37454		36	$C_0^1A_0^1$
	37456		38	$D_0^1A_0^1$
	37462		43	$V_0^1A_0^1$
	37461		51	V_0^2
	37473		54	$V_0^1D_0^1$
II				
	37467	-10	0	0_0^0
	37477		10	A_0^1
	37491		24	B_0^1
	37493		26	V_0^1
$Tol(C_3H_8)_2$ I				
	37361	-117	0	0_0^0
	37374		13	V_0^1
	37388		27	V_0^2
	37402		41	V_0^3

TABLE VI
(continued)

Species		Energy (cm^{-1})	Energy origin relative to Tol 0_0^0 (cm^{-1})	Energy relative to cluster 0_0^0 (cm^{-1})	Assignment[a]
	II				
		37436	-41	0	0_0^0
		37456		14	V_0^1
	III				
		37457	-20	0	0_0^0
		37479		22	V_0^1
	IV				
		37472	- 5	0	0_0^0
		37489		16	B_0^1
		37492		20	V_0^1
$Tol(C_3H_8)_3$	I				
		37421	-57	0	0_0^0
		37434		13	V_0^1
		37446		25	V_0^2
	II				
		37454	-24	0	0_0^0
		37469		15	A_0^1
		37477		23	V_0^1

a) A through D represent different vdW bends and V represents the fundamental vdW stretch. I through IV represent different geometries.

TABLE VII

The atomic positions for the minimum energy configurations of Tol$(C_3H_8)_1$ (see figure 9). The origin and the coordinates of the solute are the same as in Table III.

	Atom	X(Å)	Y(Å)	Z(Å)	Energy (cm^{-1})
Configuration I					-1196
Ligand	C1	- .438	0	3.418	
	C2	.819	0	4.29	
	C3	2.060	0	3.396	
	H1	-1.33	0	4.061	
	H2	- .360	.774	2.970	
	H3	- .360	- .774	2.970	
	H4	.825	.898	4.925	
	H5	.825	- .898	4.925	
	H6	2.964	0	4.023	
	H7	1.974	.774	2.950	
	H8	1.974	- .774	2.950	
Configuration II					-1128
Ligand	C1	1.521	1.248	3.617	
	C2	.638	- .001	3.636	
	C3	1.520	-1.250	3.616	
	H1	.887	2.146	3.632	
	H2	1.985	1.165	4.381	
	H3	1.951	1.166	2.834	
	H4	.020	- .001	4.424	
	H5	- .014	0	2.876	
	H6	.886	-2.148	3.629	
	H7	1.984	-1.169	4.380	
	H8	1.950	-1.168	2.832	

TABLE VIII

The atomic positions for the minimum energy geometry of configuration IV of $Tol(C_3H_8)_2$ (see figure 10). The origin and coordinates of the solute are the same as in Table III.

	Atom	X(Å)	Y(Å)	Z(Å)	Energy (cm^{-1})
Configuration IV					-2376
Ligand 1	C1	1.992	1.278	3.661	
	C2	.954	.155	3.643	
	C3	1.667	-1.198	3.633	
	H1	1.480	2.251	3.668	
	H2	2.420	1.131	4.435	
	H3	2.429	1.147	2.888	
	H4	.320	.230	4.414	
	H5	.329	.246	2.866	
	H6	.920	-2.006	3.620	
	H7	2.116	-1.183	4.410	
	H8	2.125	-1.167	2.862	
Ligand 2	C1	-2.720	.898	3.577	
	C2	-3.350	- .490	3.439	
	C3	-2.263	-1.560	3.585	
	H1	-3.502	1.665	3.472	
	H2	-2.248	.987	4.566	
	H3	-1.963	1.034	2.792	
	H4	-3.823	- .580	2.450	
	H5	-4.108	- .627	4.224	
	H6	-2.716	-2.558	3.486	
	H7	-1.505	-1.423	2.800	
	H8	-1.790	-1.471	4.574	

TABLE IX

The ratio of the solvent dimer binding energy (BE_{LL}) to the solute-solvent binding energy (BE_{SL}), the evaluation of eq(3) in the text, and the experimental intensity ratio for isotopic and anisotopic clusters. All energies are in cm^{-1} based on the calculations.

Solute	Solvent	BE_{LL}	BE_{SL}	$\frac{BE_{LL}}{BE_{SL}}$	$\exp\left(\frac{-BE_{LL}}{\frac{1}{2}BE_{SL}}\right)$	$\frac{I_{iso}}{I_{aniso}}$
toluene	methane	227	667	.34	.51	3
benzene	methane	227	589	.39	.46	1
toluene	ethane	503	926	.54	.34	.2
toluene	propane	786	1128	.70	.25	
benzene	ethane	503	778	.65	.27	0
benzene	propane	786	1040	.76	.22	0

FIGURE CAPTIONS

FIGURE 1

Two-color TOFMS of Tol$(CH_4)_1$ (upper trace) and Tol$(CH_4)_2$ in the 0_0^0 region. The energy scale is relative to the Tol 0_0^0 (37477.5 cm^{-1}). Assignments are given in Table II. This figure is reproduced from reference 5.

FIGURE 2

Two-color TOFMS of toluene-methane large clusters in the 0_0^0 region. The energy scale is relative to the Tol 0_0^0 (37477.5 cm^{-1}). The concentration of methane in the beam is 1% for Tol$(CH_4)_3$ and 2.5% for Tol$(CH_4)_4$ and Tol$(CH_4)_6$. The pulsed nozzle is cooled to 4°C and P_o = 100 psia.

FIGURE 3

Minimum energy configurations of Tol$(CH_4)_1$ and Tol$(CH_4)_2$. Atomic positions are given in Table III. Note that both isotropic (I) and anisotropic (II) clusters of Tol$(CH_4)_2$ are predicted in the computer modeling.

FIGURE 4

Two-color TOFMS of toluene-ethane clusters in the 0_0^0 region. The energy scale is relative to the Tol 0_0^0 (37477.5 cm^{-1}). The concentration of ethane in the beam is 0.5% for Tol$(C_2H_6)_1$ and Tol$(C_2H_6)_2$ and 2.0% for Tol$(C_2H_6)_3$. The backing conditions for the pulsed nozzle are P_o = 100 psia and T_o = 4°C. Data for Tol$(C_2H_6)_1$ and Tol$(C_2H_6)_2$ are presented in Table IV.

FIGURE 5

Minimum energy configurations of $Tol(C_2H_6)_1$ and $Tol(C_2H_6)_2$. Atomic positions are given in Table V. $Tol(C_2H_6)_2$ also shows isotropic and anisotropic clusters.

FIGURE 6

Two-color TOFMS of toluene-propane small clusters in the 0_0^0 region. The energy scale is relative to the Tol 0_0^0 (37477.5 cm^{-1}). The concentration of propane in the beam is 1% for all three spectra. The pulsed nozzle conditions are P_o = 100 psia and T_o = 4°C. Data for these spectra are presented in Table VI.

FIGURE 7

Two-color TOFMS of $Tol(C_3H_8)_1$ and $Tol(C_3H_8)_2$ under hot nozzle conditions. The energy scale is relative to the Tol 0_0^0 (37477.5 cm^{-1}). The concentration of propane is 1%, P_o = 40 psia and T_o 70°C. Note the dramatic increase in the background relative to the spectra in Figure 6. This broad background is due to hot bands. The negative peak at 0 cm^{-1} in the $Tol(C_3H_8)_1$ spectrum is due to detector overload at Tol 0_0^0.

FIGURE 8

Two-color TOFMS of toluene-propane large clusters. The energy scale is relative to the Tol 0_0^0. The concentration of propane in the beam is 2% and the nozzle backing conditions are P_o = 100 psia and T_o = 4°C.

FIGURE 9

Minimum energy configurations of $Tol(C_3H_8)_1$. Atomic positions are given in Table VII. In configuration II the propane interacts less with the aromatic cloud than in configuration I.

FIGURE 10

Minimum energy configurations of $Tol(C_3H_8)_2$. Only configuration IV was minimized in the computer modeling. The other configurations are composites of the geometries of $Tol(C_3H_8)_1$ shown in Figure 9. The atomic positions of configurations IV are given in Table VIII.

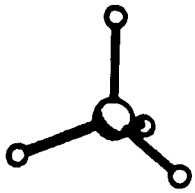

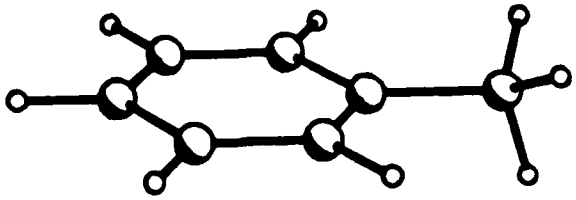

I

II

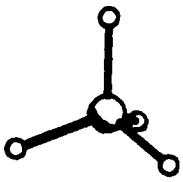

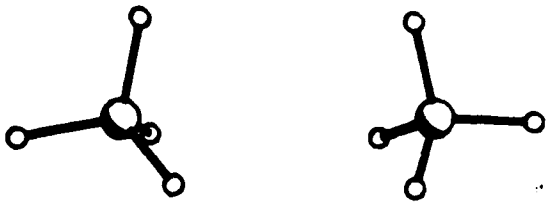

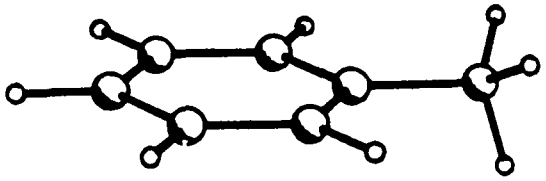

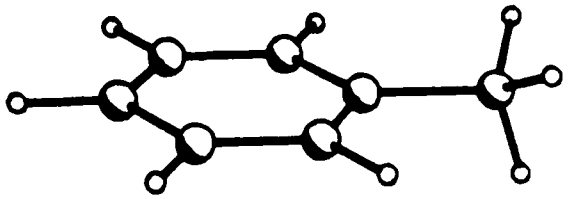

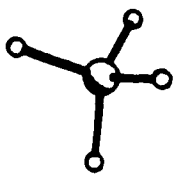

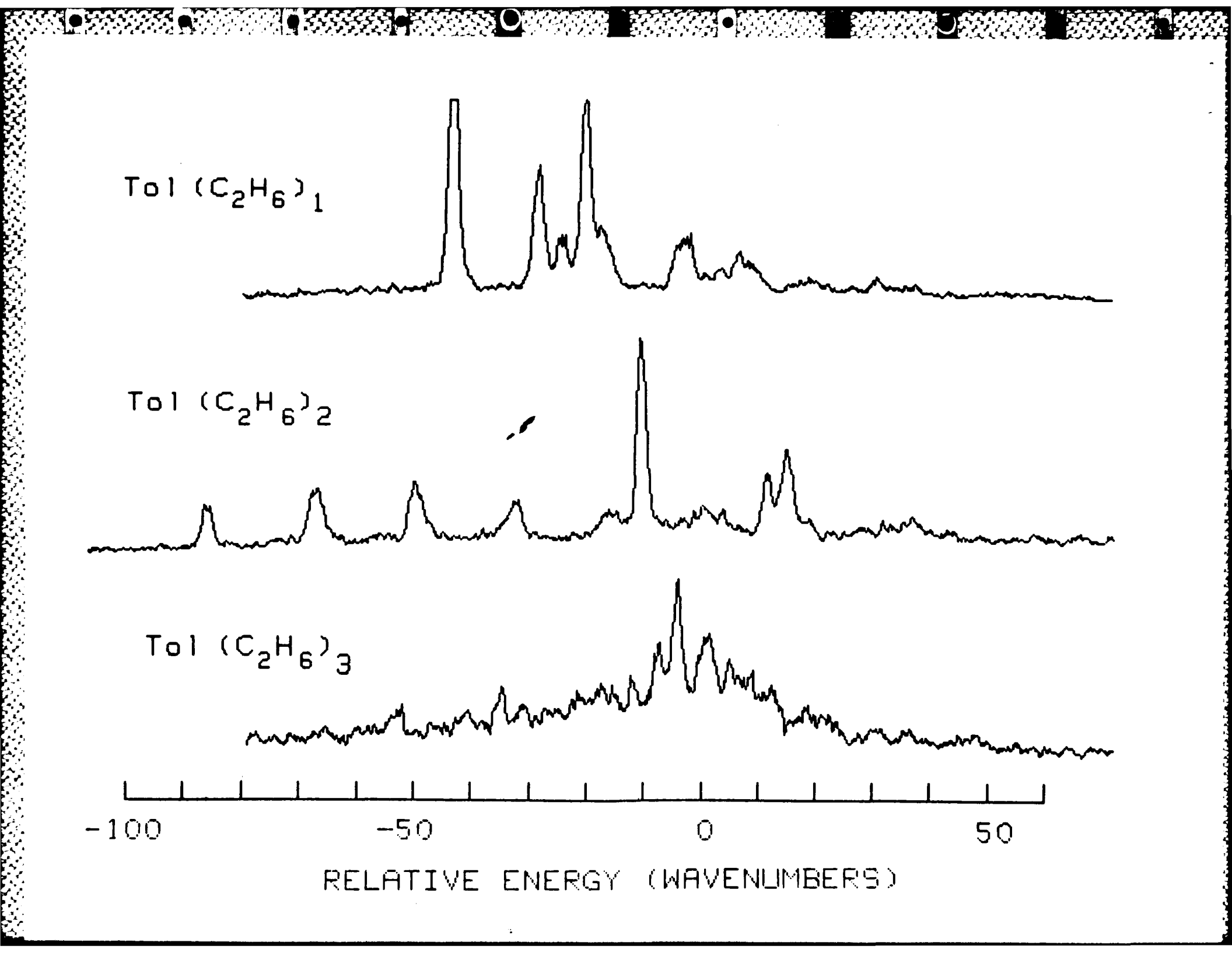
Tol $(C_2H_6)_1$
Tol $(C_2H_6)_2$
Tol $(C_2H_6)_3$
-100
-50
0
50
RELATIVE ENERGY (WAVENUMBERS)

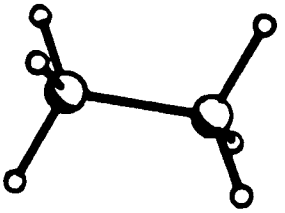

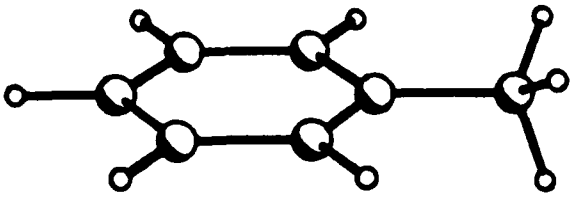

I

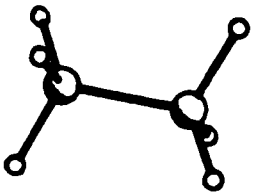

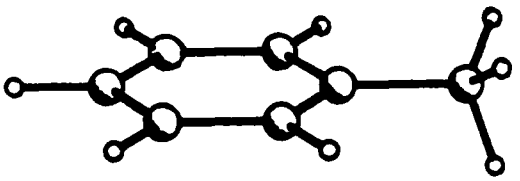

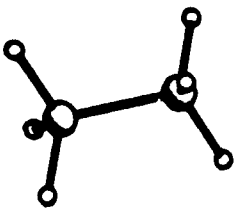

II

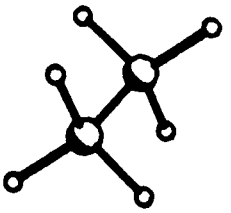

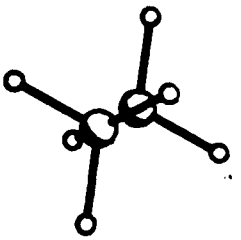

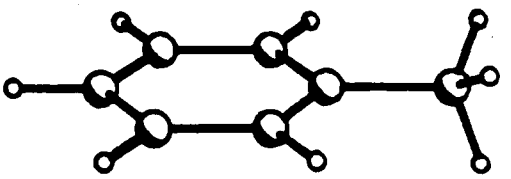

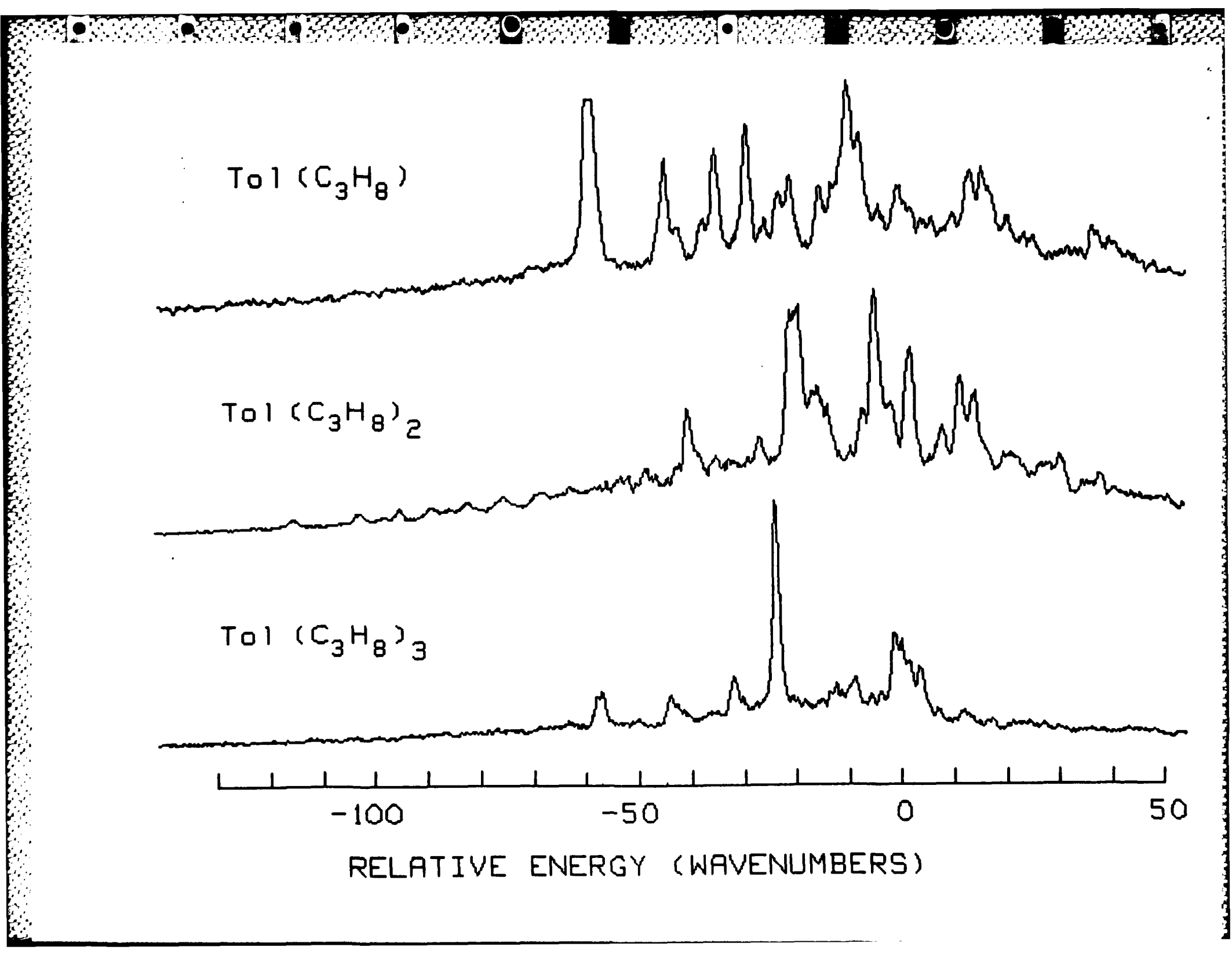
Tol (C_3H_8)
Tol $(C_3H_8)_2$
Tol $(C_3H_8)_3$
-100
-50
0
50
RELATIVE ENERGY (WAVENUMBERS)

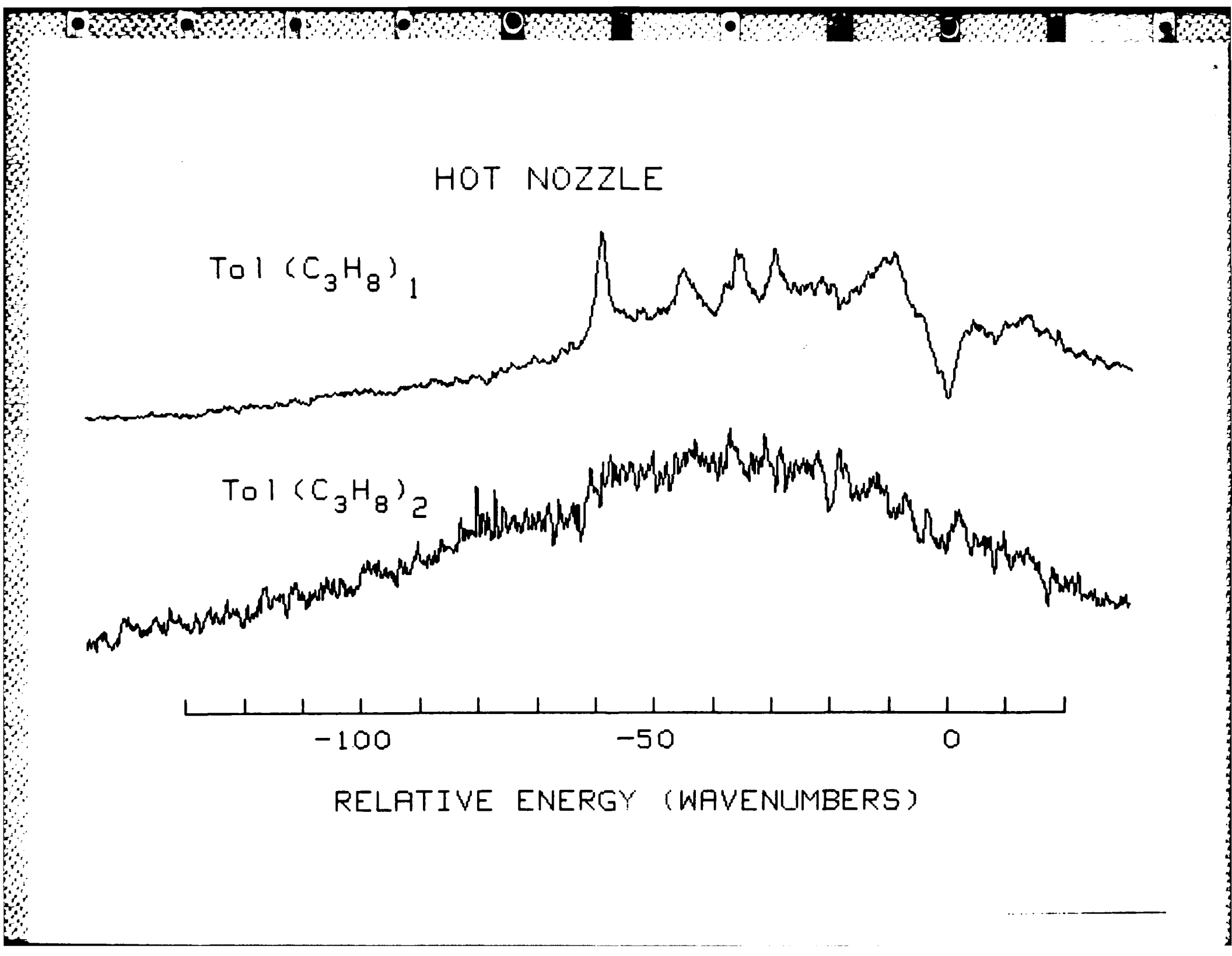
HOT NOZZLE
Tol $(C_3H_8)_1$
Tol $(C_3H_8)_2$
-100
-50
0
RELATIVE ENERGY (WAVENUMBERS)

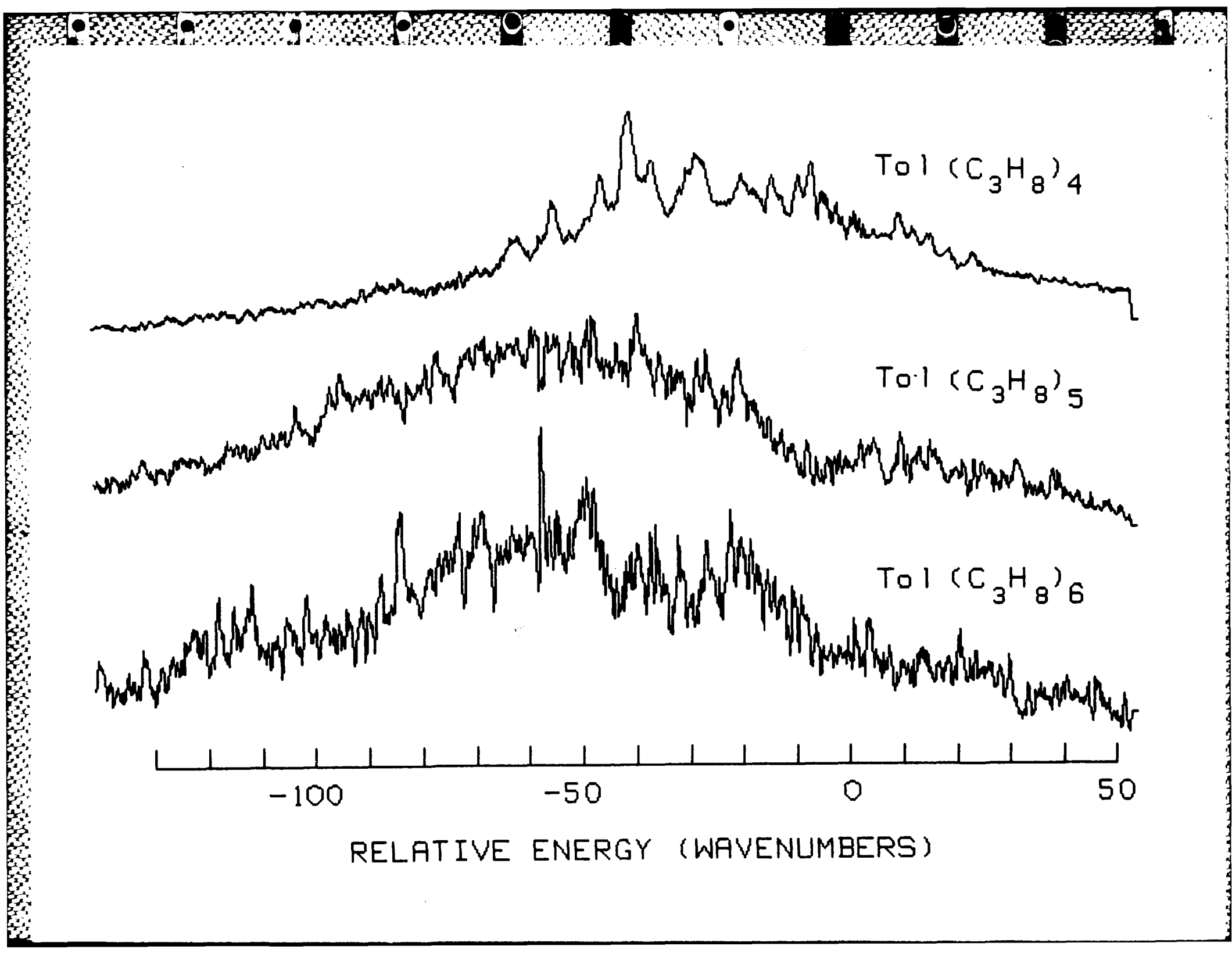
Tol $(C_3H_8)_4$
Tol $(C_3H_8)_5$
Tol $(C_3H_8)_6$
-100
-50
0
50
RELATIVE ENERGY (WAVENUMBERS)

I

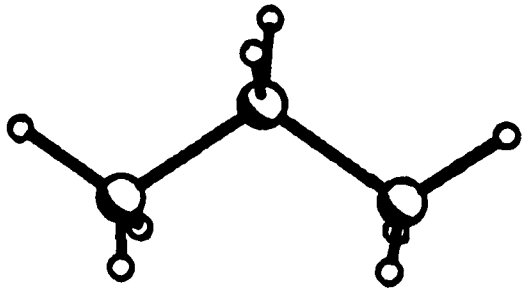

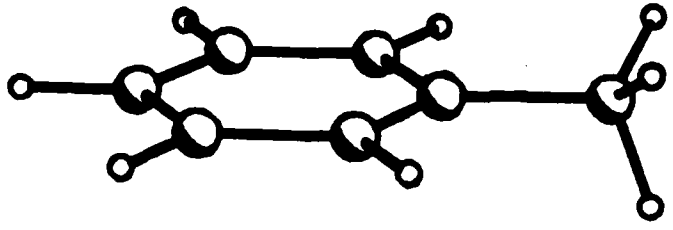

II

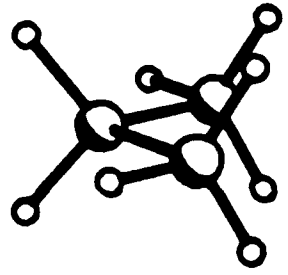

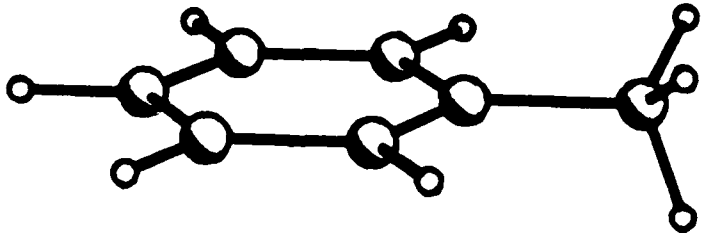

I

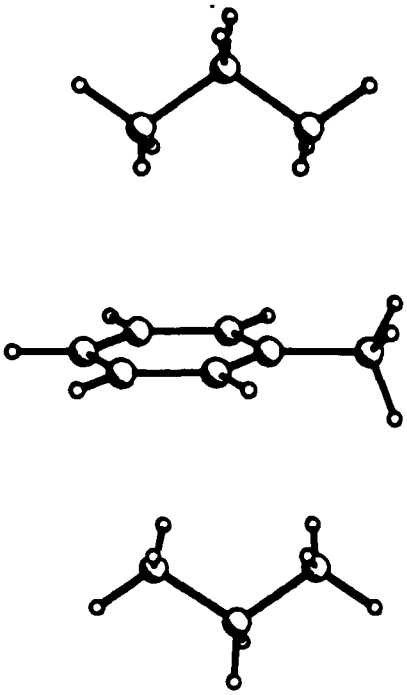

II

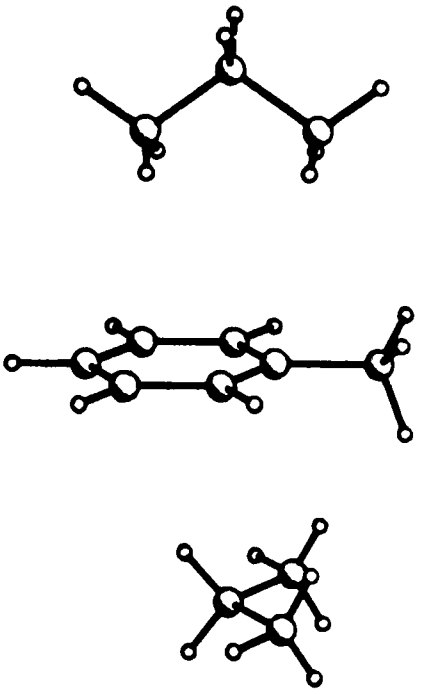

III

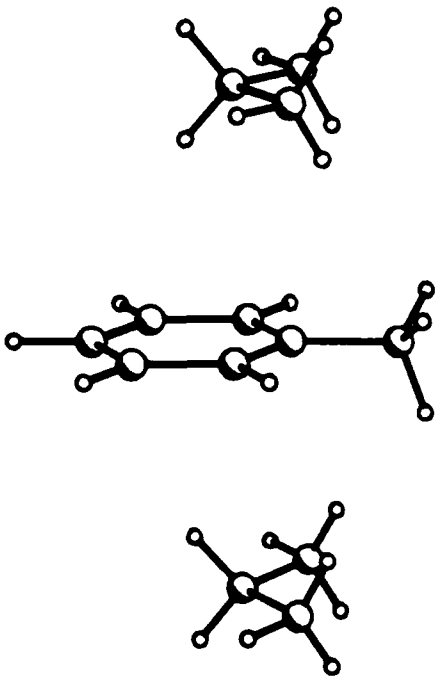

IV

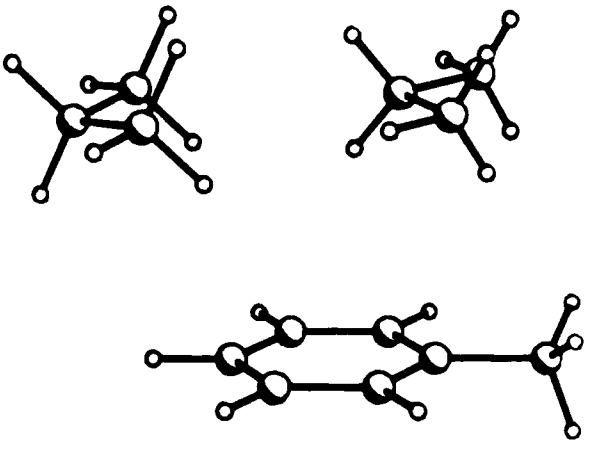

DTIC

END

4-86